

# Carbon-Aware Quality Adaptation for Energy-Intensive Services

Philipp Wiesner

Technische Universität Berlin  
Berlin, Germany  
wiesner@tu-berlin.de

Dennis Grinwald

Technische Universität Berlin &  
BIFOLD  
Berlin, Germany  
dennis.grinwald@tu-berlin.de

Philipp Weiß

Technische Universität Berlin &  
BIFOLD  
Berlin, Germany  
weiss@tu-berlin.de

Patrick Wilhelm

Technische Universität Berlin &  
BIFOLD  
Berlin, Germany  
patrick.wilhelm@tu-berlin.de

Ramin Khalili

Huawei Technologies  
Munich, Germany  
ramin.khalili@huawei.com

Odej Kao

Technische Universität Berlin  
Berlin, Germany  
odej.kao@tu-berlin.de

## Abstract

The energy demand of modern cloud services, particularly those related to generative AI, is increasing at an unprecedented pace. To date, carbon-aware computing strategies have primarily focused on batch process scheduling or geo-distributed load balancing. However, such approaches are not applicable to services that require constant availability at specific locations due to latency, privacy, data, or infrastructure constraints.

In this paper, we explore how the carbon footprint of energy-intensive services can be reduced by adjusting the fraction of requests served by different service quality tiers. We show that adapting this quality of responses with respect to grid carbon intensity can lead to additional carbon savings beyond resource and energy efficiency. Building on this, we introduce a forecast-based multi-horizon optimization that reaches close-to-optimal carbon savings and is able to automatically adapt service quality for best-effort users to stay within an annual carbon budget. Our approach can reduce the emissions of large-scale LLM services, which we estimate at multiple 10,000 tons of CO<sub>2</sub> annually, by up to 10 %.

## CCS Concepts

• **Social and professional topics** → Sustainability; • **Networks** → Cloud computing.

## Keywords

Sustainable computing, quality of service, LLM inference, green AI

## 1 Introduction

Operating modern cloud services can require substantial computing resources and energy, which directly contributes to the rapidly growing carbon footprint of computing systems [33]. Alongside traditional resource-intensive services like real-time data analytics,

This manuscript is an extended version of our paper published at *ACM e-Energy'25* (DOI: [10.1145/3679240.3734614](https://doi.org/10.1145/3679240.3734614)). Compared to the published version, we

- (1) add a time-based vs. utilization-based power attribution perspective together with a proof that both yield equivalent provisioning decisions under mild assumptions (Appendix H),
- (2) extend the online approach with an automatic adaptation of  $QoR_{target}$  to meet a fixed annual carbon budget (Sections 3.1 and 4.4).

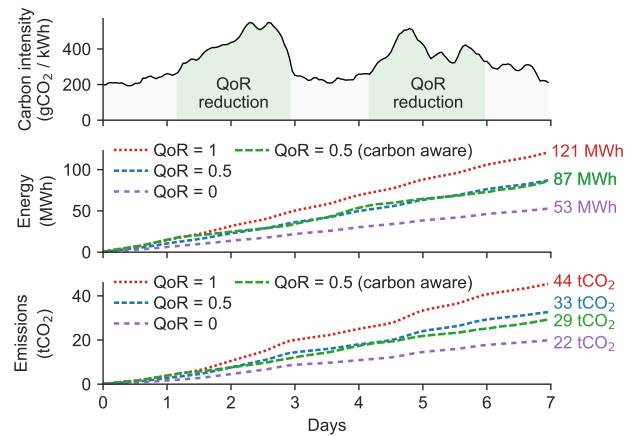


**Figure 1: We investigate how adjusting the quality of responses (QoR) with respect to carbon intensity can reduce emissions beyond savings related to reduced energy demand.**

video processing, recommendation systems, and streaming, the growing use and high energy demand of generative AI is currently driving the expansion of data centers at a high pace [2, 47]. As a result, major cloud providers, who collectively pledged to reduce their carbon footprint to zero by 2030, have been increasing their emissions significantly in recent years [9, 25, 27] and are expected to row back on sustainability commitments [17].

The concept of carbon-aware computing has emerged as a response to such challenges: Carbon-aware strategies aim to reduce emissions beyond energy efficiency by additionally taking into account how carbon-intensive the consumption of electricity at a current time and location is. Especially in the context of scheduling flexible batch workloads, the potential of temporal and spatial load shifting is well understood [13, 14, 30, 35, 43, 45, 49]. In contrast, existing carbon-aware solutions for interactive services, which handle individual requests with minimal delay-tolerance, predominantly focus on geographical load balancing [10, 28, 32, 50, 51]. However, many services cannot simply be distributed across regions due to data locality requirements, regulatory constraints, privacy and security concerns, or infrastructure limitations. Carbon-aware approaches for services that are constrained to a single region remain largely unexplored.

In this work, we focus on the *temporal* variability of carbon intensity and explain how adapting service quality with respect to this metric does not only impact energy demand, but can yield additional carbon savings. We define the quality of responses (QoR) as a type of quality of service (QoS) metric that describes the proportion of requests served by two different service quality tiers. For instance, the service quality and carbon footprint of LLM inference is determined by many factors such as the choice of model [5], quantization and pruning [21], and the number of generated tokens [20].

Figure 1 shows the accumulated energy usage and carbon emissions for an example scenario with two quality tiers over one week. Here, serving all requests at the high quality tier (QoR = 1) uses roughly twice the energy compared to serving them at the low quality tier (QoR = 0). Balancing requests evenly between the two tiers results in intermediate energy usage. We explore how strategically timing quality reductions based on carbon intensity can further reduce emissions by performing a comprehensive analysis across different regions, request patterns, and QoR constraints.

**Contributions.** Towards more carbon-efficient cloud services, we make the following contributions:

- (1) We formalize the problem of minimizing emissions under QoR constraints through optimized resource provisioning and load balancing between two service quality tiers.
- (2) We propose a forecast-based multi-horizon optimization for minimizing emissions that reaches close-to-optimal carbon savings.
- (3) We evaluate the potential and practicability of carbon-aware QoR adaptation by simulating a large-scale LLM service.

All code and data is publicly available<sup>1</sup>.

## 2 Carbon-Aware QoR Adaptation

Offering different service quality tiers is common practice in the operation of cloud services. For example, content delivery networks provide faster and more reliable service to higher-tier users, while AI platforms like OpenAI and Gemini reserve access to larger and more advanced models for paying customers. Furthermore, service providers already degrade service quality during periods of high load to prevent system overload [26, 29]. Such measures often target best-effort users: For instance, free-tier users of LLM inference services can experience highly increased latencies at certain times, to not endanger the QoS of subscribed users.

Recently, there have been proposals to design applications that can intentionally sacrifice QoS, not only to manage economical interests or load peaks, but as a strategy to improve sustainability [39, 40]. In this paper, we follow the predominant assumption that future regulations for Scope 2 emission reporting will be based on average carbon intensity (ACI), reported in carbon-equivalent emissions per unit of energy (gCO<sub>2</sub>/kWh) [10, 14, 30, 35, 43]. We examine the impact of dynamically adjusting service QoR with respect to temporal changes in ACI to enhance carbon efficiency without relying on geo-distributed load balancing.

**Problem setting.** Given an interval duration  $\Delta$ , we divide our optimization time window  $[0, T]$  into  $I = T/\Delta$  time intervals, indexed by  $i$ . For the remainder of this paper, we consider  $T = 1$  year and

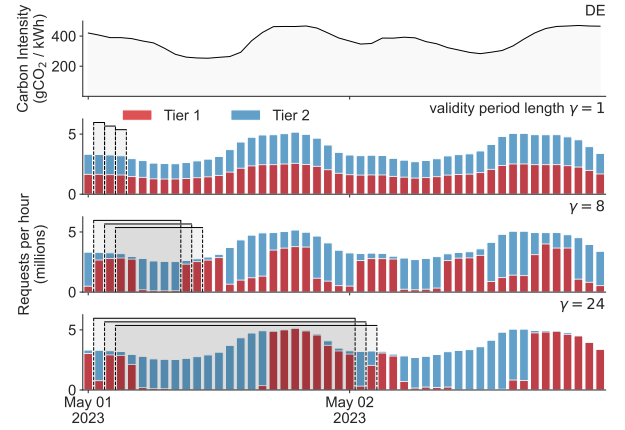


**Figure 2: Increasing validity periods allow for more flexibility in adjusting the proportion of requests served by Tier 1 and Tier 2 based on carbon intensity.**

$\Delta = 1$  hour. We define the set of user groups as  $\mathcal{U}$ , machine types  $\mathcal{M}$ , and a tuple of two service quality tiers  $\mathcal{Q} = (\text{Tier 1}, \text{Tier 2})$ . Machine types can represent physical hardware as well as virtual machines (VMs) like cloud instances. For each time interval, there is an associated carbon intensity  $C^i$  and a number of requests  $R^i$  per user group. Each machine can handle a certain number of requests by serving a certain quality tier (denoted as  $K$ ), which corresponds to its current power usage  $P^i$ . The deployment  $D^i$  must be sufficient to meet the number of incoming requests that are allocated to different service quality tiers ( $A^i$ ). The key challenge lies in determining the optimal values for both  $D^i$  and  $A^i$  for each interval. Appendix A shows an overview of all input and decision variables.

**Quality of Responses.** We define  $\text{QoR} \in [0, 1]$  as a metric that describes the proportion of requests served by two service quality tiers. That is,  $\text{QoR} = 0$  indicates that all requests are served by the lower-quality Tier 1, while  $\text{QoR} = 1$  indicates that all requests are served by the higher-quality but more energy-intensive Tier 2. When  $\text{QoR} = 0.5$ , half of the requests are served by Tier 1 and half by Tier 2. Formally, for any interval  $\cup_{i=\alpha, \dots, \omega} i$ , QoR is defined as

$$\text{QoR}(\alpha, \omega) = \frac{\sum_{i=\alpha}^{\omega} a_{u,q}^i}{\sum_{i=\alpha}^{\omega} r_u^i}, \quad (1)$$

**Validity periods.** As is typical in the assessment of QoS metrics [15], QoR is defined over validity periods of fixed length. These periods can either be disjoint (e.g., quarters, months, weeks) or, more commonly, overlapping. For the remainder of this paper, we assume that QoR is assessed over rolling windows of length  $\gamma$  (integer multiple of adjustment interval  $\Delta$ ). Staying with the above example, when the validity period is set to  $\gamma = 24$  h and we want to guarantee a specific  $\text{QoR}_{\text{target}} = 0.5$ , we have to ensure that within each 24 hour window at least 50% of all requests are served by Tier 2. Formally,  $0.5 \leq \min \{\text{QoR}(i, i + \gamma)\}_{i=\alpha}^{\omega}$ . Figure 2 illustrates how the validity period length influences the hourly QoR over time. Longer validity periods provide greater flexibility in balancing service quality in response to fluctuations in carbon intensity, but can lead to prolonged periods of high or low hourly QoR.

<sup>1</sup><https://github.com/dos-group/qualitytime>

**Carbon emission model.** We define a service's estimated carbon emissions  $E^i$  during time interval  $i$  with respect to the deployments current power usage, the region's carbon intensity  $C^i$  (in gCO<sub>2</sub>/kWh), and the attributed embodied emissions  $C_m^{\text{emb}}$  (in gCO<sub>2</sub>) for running machine  $m$  for time  $\Delta$ :

$$E^i = \sum_{m \in \mathcal{M}} \sum_{q \in \mathcal{Q}} d_{m,q}^i \left( \Delta p_{m,q}^i C^i + C_m^{\text{emb}} \right) \quad (2)$$

Depending on the methodology, embodied emissions may be excluded from scheduling decisions [3], in which case  $C_m^{\text{emb}} = 0$ . We do not explicitly model emissions per user or request in this paper, but they can be derived using carbon attribution models [12, 42].

**Time-based vs. utilization-based power attribution.** The operational emissions in (2) require a choice of how to attribute power draw to a service and its resources. Two common modeling choices are: (i) *utilization-based* power attribution, where per-machine power depends on resource utilization, and (ii) *time-based* power attribution, where every active machine is assigned a (typically constant) attributed power draw per unit time.

Utilization-based models are a natural fit when modeling operator-side electricity usage (often reported as Scope 2), where metering reflects the actual energy consumed by servers. Time-based attribution is common in tenant-side carbon accounting (often reported as Scope 3) when emissions are allocated proportional to instance-hours. However, Scope 3 methodologies can also be utilization- or energy-based, and Scope 2 reporting can rely on attributed values depending on available measurements.

For utilization-based attribution, machine power draw can be modeled as utilization-dependent, e.g., with a concave power law,

$$p_q^i = p_q^{\text{idle}} + (p_q^{\text{max}} - p_q^{\text{idle}}) \cdot (\text{util}_q^i)^n, \quad n \in (0, 1], \quad (3)$$

where, in our setting with one user group and one machine type,  $\text{util}_q^i = a_q^i / (d_q^i \cdot k_q)$ . Under time-based attribution,  $p_q^i$  is treated as utilization-independent (constant per active instance). We show that under mild concavity assumptions, optimizing under time-based vs. utilization-based attribution yields equivalent provisioning decisions (Appendix H).

**Optimization problem.** We formalize the problem of optimizing service deployments  $D^i$  that minimize carbon emissions, while providing an allocation  $A^i$  of requests to different service quality tiers that satisfies a  $\text{QoR}_{\text{target}} \in [0, 1]$ :

$$\min \sum_{i=\alpha}^{\omega} E^i \quad (4)$$

$$\text{s.t.} \quad \sum_{q \in \mathcal{Q}} a_{u,q}^i = r_u^i \quad \forall i, \forall u \quad (5)$$

$$\sum_{u \in \mathcal{U}} a_{u,q}^i \leq \sum_{m \in \mathcal{M}} d_{m,q}^i \cdot k_{m,q} \quad \forall i, \forall q \quad (6)$$

$$\text{QoR}_{\text{target}} \leq \min \{ \text{QoR}(i, i + \gamma) \}_{i=\alpha}^{\omega} \quad (7)$$

where (5) ensures that all requests during each interval  $i$  are attributed to a quality tier, (6) ensures that the provided machines have sufficient capacity to serve all requests per quality tier, and (7) ensures that the QoR of every validity period stays above  $\text{QoR}_{\text{target}}$ .

Note, that this problem is not only NP-hard (see Appendix B) but also assumes knowledge of future carbon intensity ( $C^i$ ) and requests ( $R^i$ ). As such, it cannot be solved directly in practice.

### 3 Online Approach

A practical approach for carbon-aware QoR adaptation must cope with two sources of inaccuracy:

- (1) **Approximation errors:** Optimally solving the MILP over a large solution space is computationally infeasible. In our experiments, no annual-horizon instance solved within 1 hour, while the median runtime on daily-horizon instances was 1.2 seconds (see Appendix C).
- (2) **Forecast errors:** Long-term forecasts tend to be less accurate than short-term ones, particularly in regions with volatile renewable generation [19, 23].

Based on these findings, we propose a multi-horizon optimization which periodically updates forecasts and determines an optimal (or close-to-optimal) deployment and load balancing for every interval  $i$ , described in Algorithm 1.

---

#### Algorithm 1 Multi-Horizon Optimization

---

```

1: for  $\alpha \leftarrow 0$  to  $I - 1$  do
2:   # Long-term optimization
3:   if  $\alpha \equiv 0 \pmod{\tau}$  then
4:      $(R^i, C^i)_{i=\alpha}^{I-1} \leftarrow$  update forecasts
5:      $(D^i, A^i)_{i=\alpha}^{I-1} \leftarrow \min_{(D^i, A^i)_{i=\alpha}^{I-1}} \sum_{i=\alpha}^{I-1} E^i$ 
6:   # Short-term optimization
7:    $(D^i, A^i)_{i=\alpha}^{\alpha+\gamma} \leftarrow \min_{(D^i, A^i)_{i=\alpha}^{\alpha+\gamma}} \sum_{i=\alpha}^{\alpha+\gamma} E^i$ 
8:   # Progress in time
9:   execute_interval( $D^\alpha$ )
10:   $R^\alpha, C^\alpha, D^\alpha, A^\alpha \leftarrow$  update past with observed reality

```

---

We perform the optimization in two distinct steps:

- (1) A *long-term optimization*, ensures global feasibility, i.e., meeting QoR constraints. It is executed every  $\tau$  intervals (e.g., every 24 hours) and solves the MILP for the remainder of the year. Any past  $D^i$  and  $A^i$  are fixed, so we only optimize  $(D^i, A^i)_{i=\alpha}^{I-1}$ , where  $\alpha$  is the current interval. Solutions may be approximate due to solver time limits.
- (2) A *short-term optimization* adapts to recent forecast updates and improves suboptimal long-term decisions. It is executed every interval and solves the problem within a fixed horizon<sup>2</sup>. As we only optimize over  $(D^i, A^i)_{i=\alpha}^{\alpha+\gamma}$ , this optimization has a significantly smaller search space and is more likely to find an optimal solution quickly. If no solution is found, we select an  $A^i$  such that  $\text{QoR}(\alpha, \omega) = 1$ , and determine the minimal  $D^i$  that satisfies Equation (6).

After optimization, the determined deployment  $D^\alpha$  is provisioned for the current interval. As short-term load and carbon intensity predictions are usually very precise, and the provisioning

<sup>2</sup>We found that the validity period length  $\gamma$  is a good indicator for horizon length, although it can be shorter or longer (as future values of  $A^i$  are fixed by the long-term optimization). In Line 7 we assume  $\gamma$  as the horizon.

of new nodes can take significant time (Microsoft reports 6-8 minutes for creating a new LLM inference instance [34]) we assume that there are usually no rapid auto-scaling decisions within an interval. After the interval has passed, we update the actually observed  $D^\alpha$  and  $A^\alpha$ , alongside the observed number of requests and carbon intensity.

### 3.1 Automatic QoR Adaptation under an Annual Budget

The optimization problem in Section 3 minimizes emissions under a given  $\text{QoR}_{\text{target}}$ . However, especially for best-effort users, an alternative objective is to provide the *highest possible* service quality while staying within an annual carbon budget  $B$ . This setting is relevant when operators (or tenants) face internal sustainability targets, reporting requirements, or carbon pricing that effectively turns emissions into a constrained resource.

We model this by making  $\text{QoR}_{\text{target}}$  a decision variable and optimizing

$$\max \quad \text{QoR}_{\text{target}} \quad (8)$$

$$\text{s.t.} \quad (5) - (6)$$

$$\sum_{i=\alpha}^{\omega} E^i \leq B \quad (9)$$

$$\text{QoR}_{\text{target}} \leq \min \{ \text{QoR}(i, i + \gamma) \}_{i=\alpha}^{\omega}. \quad (10)$$

In practice, when re-optimizing at time  $\alpha$ , a part of the budget has already been spent. Let  $E^0, \dots, E^{\alpha-1}$  be the (observed) emissions of past intervals. Then the remaining budget is

$$B_{\text{rem}}(\alpha) = B - \sum_{i=0}^{\alpha-1} E^i, \quad (11)$$

and the long-term optimization step is solved over the remaining horizon with  $\sum_{i=\alpha}^{\omega} E^i \leq B_{\text{rem}}(\alpha)$  while keeping all past decisions fixed. In the multi-horizon optimization (Algorithm 1), we use (8) as the objective for the long-term optimization step. This enables periodic updates of  $\text{QoR}_{\text{target}}$  based on forecast updates and already-incurred emissions, while the short-term step continues to refine per-interval decisions within a smaller horizon.

## 4 Experiments

We evaluate our approach by simulating an LLM inference service over the year 2023 using 8 real and synthetic request traces in 10 different regions. All experiments were provided 16 cores of an HPC cluster, using Gurobi [11] for optimization.

**Scenario.** We investigate an LLM inference scenario, where a single user group is served by a LLaMA 3.1 [4] model through the inference and serving engine vLLM [16]. Users can be fully served by LLaMA 3.1 8B ( $\text{QoR} = 0$ ), LLaMA 3.1 70B ( $\text{QoR} = 1$ ), or a fraction of both models ( $0 < \text{QoR} < 1$ ). We consider  $\mathcal{M} = \{\text{EC2 p4d.24xlarge}\}$ , currently the only instance type with high-performance GPUs available on AWS, and define  $p_m^{\text{attr}} = 3781.8 \text{ W}$  and  $C_m^{\text{emb}} = 135.3 \text{ gCO}_2$  based on [38]. We model the machine performance  $K$  using recent benchmarks of vLLM on a EC2 p4d.24xlarge for inference, which state a throughput of 11.57 requests per second for LLaMA 3.1 8B and 5.05 requests per second for LLaMA 3.1 70B [41].

**Request traces.** We require 4 years of hourly request traces: 3 for fitting forecasting models and 1 for the analysis itself. As such data are not publicly available for LLM inference services, we evaluate our method across a diverse set of other request traces:

- **Artificial:** A *Static* trace that assumes a constant stream of hourly requests, and a *Random* trace, where we sample hourly requests from a normal distribution.
- **Human-Generated:** Two real-world traces from unrelated domains, namely the English and German Wikipedia Pageview statistics [46], *Wiki (en)* and *Wiki (de)*, and the hourly taxi trips in New York City [36], called *Taxi*.
- **Synthetic:** Three traces generated from models fitted to Google’s Borg cluster cells [8], called *Cell B, D, and F*.

All request trace datasets and our forecast methodology are explained in detail in Appendix D.

**Carbon intensity traces.** We evaluate the potential for ten globally distributed regions:

- In Europe, we consider Germany (DE), Spain (ES), Netherlands (NL), Poland (PL), and Sweden (SE)
- In the US, we consider California (CISO), Texas (ERCOT), New York (NYISO), and the Pennsylvania-Jersey-Maryland Interconnection (PJM)
- In Australia, we consider Queensland (AU-QLD)

All carbon intensity data was provided by ElectricityMaps [24]. We normalized all time zones to align the time of day with the request traces. Our forecast methodology is explained in Appendix E.

### 4.1 Absolute Emissions

We first assess the absolute annual emissions *without* carbon-aware QoR adaption. Figure 3 shows the annual emissions for *Wiki (de)*. As expected, emissions scale linearly with  $\text{QoR}_{\text{target}}$ , but we observe large differences across regions. For example, operating the service in Sweden emits almost 27 times less carbon than in Poland.

For reference, ChatGPT, one of the biggest LLM services today, reached over 200 million active users in 2024 [31]. Assuming just 5 requests per user per day, this amounts to nearly 42 million requests per hour—two orders of magnitude more than our *Wiki (en)* trace. Assuming similar performance as Llama 3.1 70B, we estimate that *the annual operational carbon emissions of large-scale LLM service providers already exceed multiple 10,000 tCO<sub>2</sub>*.

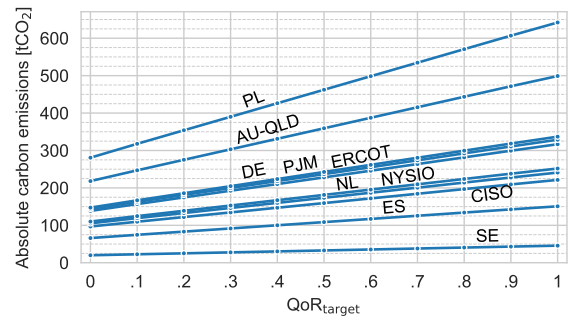


**Figure 3: Annual operational carbon emissions for *Wiki (de)* at different  $\text{QoR}_{\text{target}}$  without carbon-aware QoR adaption.**

**Table 1: Relative upper-bound carbon savings potential.**

Region	Artificial		Human-Generated			Synthetic			Mean
	Static	Rnd.	Wiki (en)	Wiki (de)	Taxi	Cell B	Cell D	Cell F	
NL	8.2	8.5	7.6	10.2	11.3	7.8	7.6	8.0	8.7±1.3
CISO	7.0	7.5	7.5	10.0	11.3	6.6	6.3	6.8	7.9±1.7
ES	7.1	7.3	6.5	9.4	10.4	6.6	6.6	6.9	7.6±1.4
AU-QLD	7.9	8.4	7.1	6.1	8.8	7.6	6.9	8.0	7.6±0.8
DE	6.3	6.7	5.7	8.7	9.7	5.9	5.8	6.1	6.9±1.4
PL	4.1	4.5	3.5	6.7	7.5	3.8	3.7	4.1	4.7±1.4
ERCOT	4.2	4.6	3.6	6.3	7.4	3.9	3.7	4.1	4.7±1.3
SE	2.7	3.0	2.0	4.9	6.1	2.3	2.2	2.6	3.2±1.4
NYISO	2.3	2.7	1.7	4.6	5.6	1.9	1.8	2.2	2.8±1.4
PJM	1.8	2.3	1.3	4.1	5.5	1.6	1.4	1.8	2.5±1.4

## 4.2 Upper-Bound Potential

To assess the potential of carbon-aware QoR adaptation, we assume perfect forecasts, and solve Equation (4) for  $\gamma = \{8 \text{ hours}, 1 \text{ day}, 1 \text{ week}, 1 \text{ month}\}$ . Shorter periods show limited potential, as ACI is reported hourly and tends to vary only slowly over time. Note, that long validity periods can lead to reduced service quality over extended periods, see Appendix G. We optimize the objective until it is within 0.1% of the optimal solution or after 1 hour.

Table 1 presents the potential for *additional* carbon savings for  $\text{QoR}_{\text{target}} = 0.5$  at  $\gamma = 1$  week. That is, instead of meeting the 50% target hourly, we ensure that 50% of requests are served by LLaMA 3.1 70B over each week. We observe that this increased flexibility enables emissions savings of around 8% in many regions. While request trace patterns exhibit little difference in potential, low-volume traces (*Wiki (de)* and *Taxi*) offer greater savings due to the larger impact of discrete scheduling decisions. For example, the volume of requests in *Wiki (de)* results in 10–25 active machines at a time, while *Wiki (en)* requires 80–200 active machines. Note, that the potential depends heavily on  $\text{QoR}_{\text{target}}$  as shown in Appendix F.

Figure 4 reports the relative and absolute saving potential for *Wiki (de)* at  $\text{QoR}_{\text{target}} = 0.5$  and different validity periods in gray. Increasing  $\gamma$  to 8 hours yields only limited additional savings—less than 3% across all settings. This is because average carbon intensity shows limited short-term variation, leaving little room for optimization. However, starting at  $\gamma = 24$  hours, we see a more notable potential of 5–8% in some regions. Regional characteristics significantly influence the expected gains: For instance, while California’s carbon intensity primarily fluctuates on a daily basis due to its heavy reliance on solar energy, Germany exhibits more complex patterns with daily, weekly, and seasonal variations [43]. As a result, extending  $\gamma$  beyond 24 hours has minimal effect in California, while in Germany, larger  $\gamma$  values lead to considerable improvements. In contrast, regions like Sweden, New York, and PJM exhibit little temporal variation in carbon intensity and have therefore a low savings potential of below 5%.

## 4.3 Potential under Realistic Conditions

We evaluate the practicability of carbon-aware QoR adaptation by applying our online approach under real forecasts (see Appendix D and E) and approximated MILP solutions: Long-term optimizations are stopped after 30s; short-term optimizations after 10s.



**Figure 4: Relative (top) and absolute (bottom) additional carbon savings for different validity periods of our proposed online approach (colored) compared to upper bound potential (gray). Larger validity periods enable higher savings.**

Figure 4 shows the gap to the upper-bound performance. Across all experiments, savings under realistic conditions reached  $82 \pm 6\%$  of the upper-bound potential. Notably, even in regions with highly unpredictable request patterns (*Random* and *Cell B, D and F*), the online optimization does not show a significant performance drop.

## 4.4 Automatic QoR Adaptation under an Annual Budget

Lastly, we evaluate the automatic adaptation of  $\text{QoR}_{\text{target}}$  introduced in Section 3.1 on *Wiki (en)* in three exemplary regions. For each region, we define an annual budget based on the resulting emissions of the corresponding upper-bound experiment for  $\gamma = 24$  hours and  $\text{QoR}_{\text{target}} = 0.5$  (Section 4.2). Consequently, under perfect forecasts, an optimal solution would maintain  $\text{QoR}_{\text{target}} \approx 0.5$  throughout the year.

**Baselines.** We compare our approach to two greedy baselines that use the same forecasts as our method:

- (1) *Greedy (constant)* divides the remaining annual budget into equal per-interval budgets and greedily selects the highest feasible per-interval quality given the current forecast. Any remaining or overspent budget is evenly distributed across the remaining intervals.
- (2) *Greedy (weighted)* follows the same approach but weights the per-interval budgets by forecasted load and carbon intensity. Weightings are updated whenever forecasts are updated.

Figure 5 shows the resulting daily QoR under realistic forecasts. Since *Greedy (constant)* does not account for fluctuations in requests or carbon intensity, the provided QoR varies significantly throughout the year. *Greedy (weighted)* is more stable but can still drift toward extreme QoR values toward the end of the year as forecast errors accumulate. In contrast, periodic long-term re-optimizations

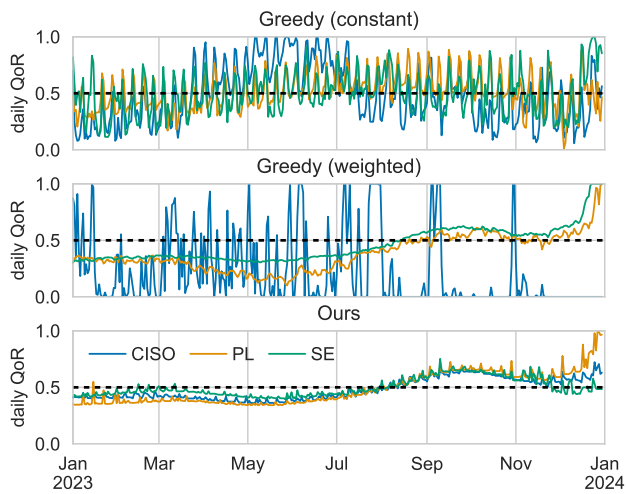


**Figure 5: Daily QoR for California (CISO), Texas (ERCOT), and Poland (PL) under an annual carbon budget. Automatic adaptation provides consistent QoR throughout the year.**

allow our approach to adjust  $QoR_{target}$  over time, yielding more consistent QoR while staying within the annual budget.

## 5 Conclusion

In this paper, we presented a first analysis of carbon-aware QoR adaptation, a strategy to reduce operational carbon emissions of cloud services without relying on geo-distributed load balancing or delay-tolerant workloads. Our results demonstrate that adjusting service quality in response to carbon intensity can reduce emissions by up to 10% beyond savings related to increased energy efficiency.

To cover a wider range of realistic settings, future work should extend our analysis to scenarios with heterogeneous machines, multiple quality tiers, and diverse user groups. It is also important to examine user-side effects, such as whether low QoR might trigger behavioral responses like repeated requests, potentially offsetting carbon savings. Additionally, future work should explore the potential of QoR adaptation under sustainability metrics used for short-term demand management, like marginal carbon intensity or excess power during curtailments [44]. These metrics exhibit higher temporal variability than average carbon intensity, potentially enabling higher savings and the use of shorter validity periods.

## Acknowledgments

This research was supported by the German Ministry for Education and Research (BMBF) as BIFOLD—Berlin Institute for the Foundations of Learning and Data (ref. BIFOLD24B), the German Research Foundation (DFG) as FONDA—Foundations of Workflows for Large-Scale Scientific Data Analysis (ref. CRC 1404), and the EU Horizon project EXIGENCE under Grant Agreement No. 101139120.

## References

- [1] Luiz André Barroso and Urs Hölzle. 2007. The Case for Energy-Proportional Computing. *IEEE Computer* 40 (2007).
- [2] Noman Bashir, Priya Donti, James Cuff, Sydney Sroka, Marija Ilic, Vivienne Sze, Christina Delimitrou, and Elsa Olivetti. 2024. The Climate and Sustainability Implications of Generative AI. *An MIT Exploration of Generative AI* (2024).
- [3] Noman Bashir, Varun Gohil, Anagha Belavadi Subramanya, Mohammad Shahradd, David Irwin, Elsa Olivetti, and Christina Delimitrou. 2024. The Sunk Carbon Fallacy: Rethinking Carbon Footprint Metrics for Effective Carbon-Aware Scheduling. In *ACM Symposium on Cloud Computing (SoCC)*. <https://doi.org/10.1145/3698038.3698542>
- [4] Abhimanyu Dubey, Abhinav Jauhri, Abhinav Pandey, Abhishek Kadian, Ahmad Al-Dahle, Aiesha Letman, Akhil Mathur, Alan Schelten, Amy Yang, Angela Fan, Anirudh Goyal, Anthony Hartshorn, Aobo Yang, Archi Mitra, Archie Sravankumar, Artem Korenev, Arthur Hinsvark, Arun Rao, Aston Zhang, and Zhiwei Zhao. 2024. *The Llama 3 Herd of Models*. Technical Report. Meta.
- [5] Ahmad Faiz, Sotaro Kaneda, Ruhan Wang, Rita Chukwunyere Osi, Prateek Sharma, Fan Chen, and Lei Jiang. 2024. LLMCarbon: Modeling the End-to-End Carbon Footprint of Large Language Models. In *12th International Conference on Learning Representations (ICLR)*.
- [6] Michael R. Garey and David S. Johnson. 1979. *Computers and Intractability: A Guide to the Theory of NP-Completeness*. W. H. Freeman and Company, San Francisco.
- [7] Sukhpal Singh Gill and Rajkumar Buyya. 2018. A Taxonomy and Future Directions for Sustainable Cloud Computing: 360 Degree View. *Comput. Surveys* 51, 5, Article 104 (2018). <https://doi.org/10.1145/3241038>
- [8] Google. 2019. Google Cluster Data Traces (version 3). <https://github.com/google/cluster-data>. Accessed: 2025-01-16.
- [9] Google. 2024. 2024 Environmental Report.
- [10] Viktor Gsteiger, Daniel Long, Jerry Sun, Parshan Javanrood, and Mohammad Shahradd. 2024. Caribou: Fine-Grained Geospatial Shifting of Serverless Applications for Sustainability. In *30th Symposium on Operating Systems Principles (SOSP)*. <https://doi.org/10.1145/3694715.3695954>
- [11] Gurobi Optimization, LLC. 2024. Gurobi Optimizer Reference Manual. <https://www.gurobi.com>
- [12] Leo Han, Jash Kakadia, Benjamin C. Lee, and Udit Gupta. 2024. Towards Game-Theoretic Approaches to Attributing Carbon in Cloud Data Centers. In *3rd Workshop on Sustainable Computer Systems (HotCarbon)*.
- [13] Walid A. Hanafy, Qianlin Liang, Noman Bashir, David Irwin, and Prashant Shenoy. 2024. CarbonScaler: Leveraging Cloud Workload Elasticity for Optimizing Carbon-Efficiency. *Proceedings of the ACM on Measurement and Analysis of Computing Systems* 7, 3 (2024). <https://doi.org/10.1145/3673660.3655048>
- [14] Walid A. Hanafy, Qianlin Liang, Noman Bashir, Abel Souza, David Irwin, and Prashant Shenoy. 2024. Going Green for Less Green: Optimizing the Cost of Reducing Cloud Carbon Emissions. In *ASPLOS. ACM*. <https://doi.org/10.1145/3620666.3651374>
- [15] Alexander Keller and Heiko Ludwig. 2003. The WSLA Framework: Specifying and Monitoring Service Level Agreements for Web Services. *Journal of Network and Systems Management* 11 (2003), 57–81. <https://doi.org/10.1023/A:1022445108617>
- [16] Woosuk Kwon, Zhuohan Li, Siyuan Zhuang, Ying Sheng, Lianmin Zheng, Cody Hao Yu, Joseph E. Gonzalez, Hao Zhang, and Ion Stoica. 2023. Efficient Memory Management for Large Language Model Serving with PagedAttention. In *29th Symposium on Operating Systems Principles (SOSP)*.
- [17] Andy Lawrence. 2024. When Net-Zero Goals Meet Harsh Realities. <https://journal.uptimeinstitute.com/when-net-zero-goals-meet-harsh-realities/>
- [18] Adam Lechowicz, Nicolas Christianson, Bo Sun, Noman Bashir, Mohammad Hajjesmaili, Adam Wierman, and Prashant Shenoy. 2024. CarbonClipper: Optimal Algorithms for Carbon-Aware Spatiotemporal Workload Management. *arXiv preprint arXiv: 2408.07831* (2024).
- [19] Amy Li, Sihang Liu, and Yi Ding. 2024. Uncertainty-Aware Decarbonization for Datacenters. In *3rd Workshop on Sustainable Computer Systems (HotCarbon)*.
- [20] Baolin Li, Yankai Jiang, Vijay Gadepally, and Devesh Tiwari. 2024. Sprout: Green Generative AI with Carbon-Efficient LLM Inference. In *Conference on Empirical Methods in Natural Language Processing (EMNLP)*. <https://doi.org/10.18653/v1/2024.emnlp-main.1215>
- [21] Tailin Liang, John Glossner, Lei Wang, Shaobo Shi, and Xiaotong Zhang. 2021. Pruning and quantization for deep neural network acceleration: A survey. *Neurocomputing* 461 (2021), 370–403. <https://doi.org/10.1016/j.neucom.2021.07.045>
- [22] Zinan Lin, Alankar Jain, Chen Wang, G. Fanti, and Vyas Sekar. 2019. Using GANs for Sharing Networked Time Series Data: Challenges, Initial Promise, and Open Questions. *ACM/SIGCOMM Internet Measurement Conference* (2019). <https://doi.org/10.1145/3419394.3423643>
- [23] Diptyaroop Maji, Prashant Shenoy, and Ramesh K. Sitaraman. 2023. Multi-Day Forecasting of Electric Grid Carbon Intensity Using Machine Learning. *SIGENERGY Energy Informatics Review* 3, 2 (2023), 19–33. <https://doi.org/10.1145/3607114.3607117>
- [24] Electricity Maps. 2024. Electricity Maps Data Portal – Carbon Intensity Data. <https://www.electricitymaps.com/data-portal>
- [25] Inc. Meta Platforms. 2023. 2023 Sustainability Report. <https://sustainability.fb.com/reports/2023-sustainability-report> Accessed: 2024-10-07.
- [26] Justin J. Meza, Thote Gowda, Ahmed Eid, Tomiwa Ijaware, Dmitry Chernyshev, Yi Yu, Md Nazim Uddin, Rohan Das, Chad Nachiappan, Sari Tran, Shuyang Shi, Tina Luo, David Ke Hong, Sankaralingam Panneerselvam, Hans Ragas, Svetlin Manavski, Weidong Wang, and Francois Richard. 2023. Defcon: Preventing

- Overload with Graceful Feature Degradation. In *17th USENIX Symposium on Operating Systems Design and Implementation (OSDI)*.
- [27] Microsoft. 2024. 2024 Environmental Sustainability Report.
- [28] Jorge Murillo, Walid A. Hanafy, David Irwin, Ramesh Sitararam, and Prashant Shenoy. 2024. CDN-Shifter: Leveraging Spatial Workload Shifting to Decarbonize Content Delivery Networks. In *ACM Symposium on Cloud Computing (SoCC)*. <https://doi.org/10.1145/3698038.3698516>
- [29] Jinwoo Park, Jaehyeong Park, Youngmok Jung, Hwijoon Lim, Hyunho Yeo, and Dongsu Han. 2024. TopFull: An Adaptive Top-Down Overload Control for SLO-Oriented Microservices. In *ACM SIGCOMM Conference*. 876–890. <https://doi.org/10.1145/3651890.3672253>
- [30] Ana Radovanovic, Ross Konigstein, Ian Schneider, Bokan Chen, Alexandre Duarte, Binz Roy, Diyuexiao, Maya Haridasan, Patrick Hung, Nick Care, Saurav Talukdar, Eric Mullen, Kendal Smith, Mariellen Cottman, and Walfredo Cirne. 2022. Carbon-Aware Computing for Datacenters. *IEEE Transactions on Power Systems* 38, 2 (2022). <https://doi.org/10.1109/TPWRS.2022.3173250>
- [31] Reuters. 2024. *OpenAI says ChatGPT's weekly users have grown to 200 million*. <https://www.reuters.com/technology/artificial-intelligence/openai-says-chatgpts-weekly-users-have-grown-200-million-2024-08-29/> Accessed: 2024-10-17.
- [32] Abel Souza, Shruti Jasoria, Basundhara Chakrabarty, Alexander Bridgwater, Axel Lundberg, Filip Skogh, Ahmed Ali-Eldin, David Irwin, and Prashant J. Shenoy. 2023. CASPER: Carbon-Aware Scheduling and Provisioning for Distributed Web Services. In *International Green and Sustainable Computing Conference*. <https://doi.org/10.1145/3634769.3634812>
- [33] S&P Global Market Intelligence. 2023. 2024 Trends in Datacenter Services & Infrastructure. *451 Research 2024 Preview* (2023).
- [34] Jovan Stojkovic, Chaojie Zhang, Ínigo Goiri, Josep Torrellas, and Esha Choukse. 2024. DynamoLLM: Designing LLM Inference Clusters for Performance and Energy Efficiency. *arXiv preprint arXiv: 2408.00741* (2024).
- [35] Thanathorn Sukprasert, Abel Souza, Noman Bashir, David Irwin, and Prashant Shenoy. 2024. On the Limitations of Carbon-Aware Temporal and Spatial Workload Shifting in the Cloud. In *19th European Conference on Computer Systems (EuroSys)*. <https://doi.org/10.1145/3627703.3650079>
- [36] New York City Taxi and Limousine Commission. 2025. TLC Trip Record Data. <https://www.nyc.gov/site/tlc/about/tlc-trip-record-data.page> Accessed: 2025-01-16.
- [37] Sean Taylor and Benjamin Letham. 2017. Forecasting at scale. <https://doi.org/10.7287/peerj.preprints.3190v2>
- [38] Teads Engineering. 2024. Carbon footprint estimator for AWS instances. <https://engineering.teads.com/sustainability/carbon-footprint-estimator-for-aws-instances/> Accessed: 2024-10-15.
- [39] Monica Vitali. 2022. Towards Greener Applications: Enabling Sustainable-aware Cloud Native Applications Design. In *Advanced Information Systems Engineering*. Springer.
- [40] Monica Vitali, Paul Schmiedmayer, and Valentin Bootz. 2023. Enriching Cloud-native Applications with Sustainability Features. In *2023 IEEE International Conference on Cloud Engineering (IC2E)*. <https://doi.org/10.1109/IC2E59103.2023.00011>
- [41] vLLM Team. [n. d.]. vLLM Performance Benchmark. <https://buildkite.com/vllm/performance-benchmark/builds/8710>.
- [42] Richard Westerhof, Richard Atherton, and Vasilios Andrikopoulos. 2023. An Allocation Model for Attributing Emissions in Multi-tenant Cloud Data Centers. arXiv:2305.10439 [cs]. <http://arxiv.org/abs/2305.10439>
- [43] Philipp Wiesner, Ilja Behnke, Dominik Scheinert, Kordian Gontarska, and Lauritz Thamsen. 2021. Let's Wait Awhile: How Temporal Workload Shifting Can Reduce Carbon Emissions in the Cloud. In *ACM/IFIP International Middleware Conference*. <https://doi.org/10.1145/3464298.3493399>
- [44] Philipp Wiesner and Odej Kao. 2025. Moving Beyond Marginal Carbon Intensity: A Poor Metric for Both Carbon Accounting and Grid Flexibility. In *Workshop on Measurements, Modeling, and Metrics for Carbon-Aware Computing (Carbon-Metrics) at SIGMETRICS'25*.
- [45] Philipp Wiesner, Ramin Khalili, Dennis Grinwald, Pratik Agrawal, Lauritz Thamsen, and Odej Kao. 2024. FedZero: Leveraging Renewable Excess Energy in Federated Learning. In *ACM International Conference on Future and Sustainable Energy Systems (e-Energy)*. <https://doi.org/10.1145/3632775.3639589>
- [46] Inc. Wikimedia Foundation. [n. d.]. Wikipedia Analytics Datasets: Pageviews. <https://dumps.wikimedia.org/other/pageviews>.
- [47] Carole-Jean Wu, Bilge Acun, Ramya Raghavendra, and Kim Hazelwood. 2024. Beyond Efficiency: Scaling AI Sustainably. *IEEE Micro* (2024), 1–8. <https://doi.org/10.1109/MM.2024.3409275>
- [48] Minxian Xu, Wenhong Tian, and Rajkumar Buyya. 2017. A survey on load balancing algorithms for virtual machines placement in cloud computing. *Concurrency and Computation: Practice and Experience* 29, 12 (2017). <https://doi.org/10.1002/cpe.4123>
- [49] Jijia Zheng, Andrew A. Chien, and Sangwon Suh. 2020. Mitigating Curtailment and Carbon Emissions through Load Migration between Data Centers. *Joule* 4,

- 10 (2020).
- [50] Zhi Zhou, Fangming Liu, Yong Xu, Ruolan Zou, Hong Xu, John C.S. Lui, and Hai Jin. 2013. Carbon-Aware Load Balancing for Geo-distributed Cloud Services. *IEEE 21st International Symposium on Modelling, Analysis and Simulation of Computer and Telecommunication Systems (MASCOTS)* (2013), 232–241. <https://doi.org/10.1109/MASCOTS.2013.31>
- [51] Zhi Zhou, Fangming Liu, Ruolan Zou, Jiangchuan Liu, Hong Xu, and Hai Jin. 2016. Carbon-Aware Online Control of Geo-Distributed Cloud Services. *IEEE Transactions on Parallel and Distributed Systems* 27 (2016), 2506–2519. <https://doi.org/10.1109/TPDS.2015.2504978>

## A Nomenclature

**Table 2: Description of symbols. Small letters denote the elements of the corresponding, capitalized matrix.**

Input variables	
$\mathcal{U}$	Set of user groups $u$
$\mathcal{M}$	Set of machine types $m$
$\mathcal{Q}$	Tuple of two service quality tiers $q$
$\gamma \in \mathbb{N}$	Validity period length
$R^i \in \mathbb{R}^{ \mathcal{U} }$	Number of requests ( $r_u^i$ ) for user group $u$ during $i$ .
$C^i \in \mathbb{R}$	Carbon intensity during $i$ .
$P^i \in \mathbb{R}^{ \mathcal{Q}  \times  \mathcal{M} }$	Power usage ( $p_{m,q}^i$ ) of machine $m$ serving quality $q$ during $i$ .
$K \in \mathbb{R}^{ \mathcal{Q}  \times  \mathcal{M} }$	Requests per interval ( $k_{m,q}$ ) that machine $m$ can serve at quality $q$ .
$C_m^{\text{emb}} \in \mathbb{R}$	Attributed embodied emissions for running machine $m$ for time $\Delta$ .
Decision variables	
$D^i \in \mathbb{N}^{ \mathcal{Q}  \times  \mathcal{M} }$	Deployment ( $d_{m,q}^i$ ), i.e., the number of machines $m$ running quality $q$ during $i$ .
$A^i \in \mathbb{R}^{ \mathcal{U}  \times  \mathcal{Q} }$	Number of requests ( $a_{u,q}^i$ ) served by quality $q$ for user group $u$ during $i$ .

## B Proof of NP-Hardness

We prove that the optimization problem defined in Equations (4)–(7) is NP-hard via a polynomial-time reduction from the *Bin Packing problem*, which is known to be NP-complete [6]. Bin Packing is defined as: *Given a set of items with sizes  $a_j \in (0, 1]$  and an integer  $B$ , can the items be packed into at most  $B$  bins of capacity 1?*

Consider a simplified instance of our problem with a single interval  $i$ , one user group  $u$ , one machine type  $m$ , and one quality tier  $q$ . Each machine has capacity  $k_{m,q} = 1$ . Requests correspond exactly to Bin Packing items, each with size  $a_j$ , and the total request volume is  $\sum_j a_j$ . In this setting, determining feasibility under Constraints (5) and (6) is equivalent to solving the Bin Packing problem: each machine corresponds to a bin, each request to an item, and the capacity constraint ensures that the sum of assigned request sizes per machine does not exceed 1. Since this special case of our problem is equivalent to Bin Packing, and Bin Packing is NP-complete, it follows that our optimization problem is NP-hard.  $\square$

## C Performance Analysis

To illustrate the performance improvements achieved by the proposed multi-horizon optimization, we analyze 240 experiments (all regions, all trace datasets, and  $\text{QoR}_{\text{target}} \in \{0.3, 0.5, 0.7\}$ ) for the annual-horizon and daily-horizon optimization. These correspond

to the long-term and short-term optimization components of our evaluated online approach.

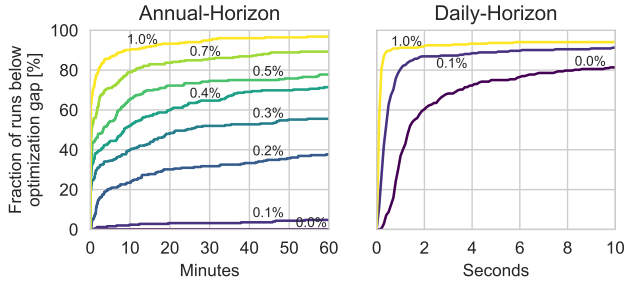


Figure 6: CDF of optimization gap over time.

Figure 6 shows a CDF over the fraction of runs below a certain optimization gap over time. In the annual-horizon optimization, around 10% of all runs have not found a solution within 1% of the optimum within 10 minutes, while no run found an optimal solution within one hour. In the daily-horizon optimization, the median runtime was only 1.2 seconds and more than 80% of all runs found an optimal solution within 10 seconds.

## D Request Traces

This section describes all request trace datasets used in the experiments. Table 3 presents summary statistics.

Table 3: Request trace and 24-hour forecast statistics.

	Dataset statistics ( $1 \times 10^6$ )			Forecast statistics
	Mean $\pm$ Std Dev	Min	Max	MAPE
Static	1.00 $\pm$ 0.00	1.00	1.00	0.0 $\pm$ 0.0
Normal	1.00 $\pm$ 0.34	0.00	2.36	38.6 $\pm$ 24.6
Wiki (en)	3.38 $\pm$ 0.80	1.88	16.41	13.9 $\pm$ 8.4
Wiki (de)	0.42 $\pm$ 0.24	0.04	1.56	32.1 $\pm$ 15.3
Taxi	0.33 $\pm$ 0.14	0.04	0.71	26.5 $\pm$ 7.1
Cell B	1.94 $\pm$ 0.61	0.73	4.10	27.2 $\pm$ 13.5
Cell D	2.87 $\pm$ 0.80	1.02	7.76	22.1 $\pm$ 15.8
Cell F	1.58 $\pm$ 0.41	0.87	4.32	18.2 $\pm$ 9.3

**Artificial Datasets.** We artificially create two traces:

- *Static* assumes a constant stream of  $1 \times 10^6$  hourly requests.
- *Random* comprises points randomly sampled from a normal distribution with a mean of  $\mu = 1 \times 10^6$  and a standard deviation of  $\sigma = 0.33 \times 10^6$ .

During online optimization, we always assume the mean of  $1 \times 10^6$  requests per hour as forecasts.

**Real Datasets.** We create three traces based on real data:

- *Wiki (en)* is based on the Wikipedia pageview statistics [46], namely all hourly requests to [en.wikipedia.org](https://en.wikipedia.org).
- *Wiki (de)* represents all requests to [de.wikipedia.org](https://de.wikipedia.org). The trace differs notably from *Wiki (en)*, as the German Wikipedia is primarily accessed from a single timezone, while the English Wikipedia sees traffic from around the globe.

Table 4: Carbon intensity forecast MAPE over 96 hours as reported in CarbonCast [23]

Region	Day 1	Day 2	Day 3	Day 4
CISO	8.08	11.19	12.93	13.62
PJM	3.69	4.93	5.87	6.67
ERCOT	9.78	10.93	11.61	12.23
NYISO	6.91	9.06	9.95	10.42
SE	4.29	5.64	6.43	6.74
DE	7.81	10.69	12.80	15.55
PL	3.12	4.14	4.72	5.50
ES	10.12	16.00	19.37	21.12
NL	6.06	7.87	9.08	9.99
AU-QLD	3.93	3.98	4.06	5.87

- *Taxi* is based on hourly aggregates of taxi trips in New York City [36]. We sum over all trip records (Yellow Taxi, Green Taxi, For-Hire Vehicle, High Volume For-Hire Vehicle) and multiply the events by factor 10, to bring them into a similar range with the other datasets.

To simulate realistic forecasts, we are using using Prophet [37], a state-of-the-art forecasting model that fits daily, weekly, and annual seasonalities. In particular, we fit a model every day at midnight using 3 years of historical data to forecast the rest of the year. The predictions exhibit realistic errors, denoted in Table 3.

**Synthetic Datasets.** As all real datasets exhibit very periodic patterns, we additionally created three synthetic datasets to demonstrate that carbon-aware QoR adaptation is feasible on highly unpredictable traces. For this, we aggregated the instance events of the Google cluster traces (version 3) [8] individually for the eight available Borg cells. Data was retrieved via the GoogleSQL query:

```
SELECT
  TIMESTAMP_TRUNC(TIMESTAMP_MICROS(time), HOUR) AS hour,
  COUNT(*) AS num_events
FROM `google.com:google-cluster-data.<TABLE>`
-- Exclude invalid values
WHERE time > 0 AND time < 9223372036854775807
GROUP BY hour
ORDER BY hour;
```

where `<TABLE>` is substituted by the name of the cell. For example, for cell A: "clusterdata\2019\a.instance\events".

We identified the three traces with the lowest 24-hour auto-correlation coefficients, i.e. the traces that exhibit the least daily seasonality: *Cell B* (0.17), *Cell D* (0.27), and *Cell F* (0.22). Since the Google cluster dataset only covers one month of data, we fit a DoppelGANger [22] model for each of the traces, which is a state-of-the-art GAN for timeseries generation, and generate 4 years of synthetic data per cell. We apply the same forecasting methodology that is used for real datasets.

## E Carbon Intensity Forecasts

For long-term carbon intensity forecasts, we apply the same forecasting methodology that is used for the request trace datasets. As in [18], we generate synthetic short-term forecasts of up to 4 days by adding Gaussian noise to the actually observed carbon intensity

data to match the MAPEs reported by the state-of-the-art forecasting model CarbonCast [23] for each region, see Table 4. Short-term forecasts are updated daily at midnight.

## F Impact of $QoR_{\text{target}}$

Figure 7 shows the potential for relative savings across different  $QoR_{\text{target}}$  and validity periods, for *Wiki (en)* in Germany and California. At  $QoR_{\text{target}} = 0$  and  $QoR_{\text{target}} = 1$ , we serve all requests using either LLaMA 3.1 8B or 70B, leaving no flexibility for additional savings. A  $QoR_{\text{target}}$  around 0.5 offers the greatest flexibility for carbon-aware QoR adaptation, resulting in the highest potential for carbon savings.

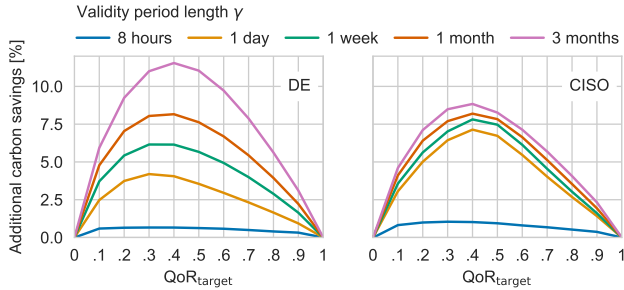


Figure 7: Additional relative savings for different  $QoR_{\text{target}}$ .

## G Periods of Low Service Quality

While increasing  $\gamma$  enhances potential for carbon savings, it also increases the probability of prolonged periods with low QoR, illustrated in Figure 8. For example, when optimizing for  $QoR_{\text{target}} = 0.5$  at  $\gamma = 1$  week, no 1-week interval has a QoR below 0.5 (right). However, 10% of all daily intervals exhibit a  $QoR_{\text{target}} < 0.48$  (left). We observe that for  $\gamma = 3$  months, users can experience multiple consecutive days of low QoR. Consequently, large validity periods are not practical in many real-world scenarios.

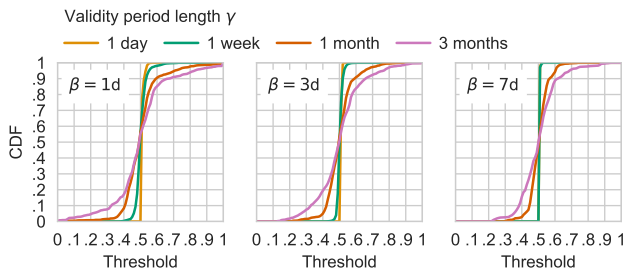


Figure 8: CDF for *Wiki (en)* in Germany at  $QoR_{\text{target}} = 0.5$ : What proportion of time intervals of length  $\beta = \{1, 3, 7\}$  days have a QoR below the threshold?

## H Equivalence of Provisioning Under Time- vs. Utilization-based Power Attribution

We prove that the optimal provisioning decision is the same under (i) utilization-based power attribution (3), where per-machine power depends on resource utilization, and (ii) time-based power

attribution, where each active machine is assigned a utilization-independent attributed power draw. This is important, as utilization-based power attribution introduces a non-linear relationship by multiplying values within  $D^i$  and  $A^i$ . This would turn the MILP into a mixed-integer quadratic program, which is considerably harder to solve.

**ASSUMPTION 1.**  $p_{m,q}^{\max} > p_m^{\text{idle}} > 0$ . This reflects the basic property that active machines consume more power under load than when idle or turned off.

**ASSUMPTION 2.**  $n \leq 1$ , i.e. the power model is concave, which is a common assumption for computing hardware as servers run more efficiently under high load [1, 7, 48].

**ASSUMPTION 3.**  $p_{m_1}^{\text{idle}} < p_{m_2}^{\text{idle}} \Rightarrow p_{m_1,q}^{\max} < p_{m_2,q}^{\max} \quad \forall m_1, m_2 \in \widehat{\mathcal{M}}$ . If a quality tier can be deployed on different machine types  $\widehat{\mathcal{M}}$ , we assume a strict ordering of these machines based on their idle and max power usage.

**THEOREM 1.** Let Assumptions 1, 2, and 3 hold. When minimizing (4) subject to (5) – (7), the utilization-based power attribution,

$$p_{m,q}^i = p_m^{\text{idle}} + (p_{m,q}^{\max} - p_m^{\text{idle}}) \cdot (util_q^i)^n,$$

can be simplified to the same form as the time-based attribution

$$\tilde{p}_{m,q}^i = p_{m,q}^{\max},$$

as it always yields an equivalent optimal deployment  $D^i$ .

**LEMMA 1.** Increasing the utilization of machines does not result in additional penalties, so there is no incentive to deploy more machines of the same type than strictly necessary. Formally, if Assumptions 1 and 2 hold, utilization-based attribution  $f$  is strictly subadditive

$$f(x + y) < f(x) + f(y), \quad (12)$$

where  $x$  and  $y$  represent utilization levels  $util_q^i \in (0, 1]$ .

**PROOF OF LEMMA 1.** We show that  $f$  is strictly subadditive for the two cases  $n = 1$  and  $n < 1$ .

*Case 1: Linear power model ( $n = 1$ ):*

$$f(x + y) = p_m^{\text{idle}} + (p_{m,q}^{\max} - p_m^{\text{idle}}) \cdot (x + y) \quad (13)$$

$$f(x + y) = p_m^{\text{idle}} + (p_{m,q}^{\max} - p_m^{\text{idle}}) x + p_m^{\text{idle}} + (p_{m,q}^{\max} - p_m^{\text{idle}}) y - p_m^{\text{idle}} \quad (14)$$

$$f(x + y) = f(x) + f(y) - p_m^{\text{idle}} \quad (15)$$

$$f(x + y) < f(x) + f(y) \quad (16)$$

*Case 2: Sub-linear power model ( $n < 1$ ):* For a strictly concave function  $f$  with  $f(0) \geq 0$ ,  $f$  is strictly subadditive on  $(0, \infty)$ .

$$f(x) = p_m^{\text{idle}} + (p_{m,q}^{\max} - p_m^{\text{idle}}) \cdot x^n \quad (17)$$

$$f'(x) = n (p_{m,q}^{\max} - p_m^{\text{idle}}) \cdot x^{n-1} \quad (18)$$

$$f''(x) = n(n-1) (p_{m,q}^{\max} - p_m^{\text{idle}}) \cdot x^{n-2} < 0 \quad (19)$$

$$f''(x) < 0 \Rightarrow \underbrace{f''(x)}_{<1} > \underbrace{f''(x)}_{>1} > \underbrace{f''(x)}_{>1} \quad (20)$$

Additionally,  $f(0) = p_m^{\text{idle}} > 0$ .  $\square$

PROOF OF THEOREM 1. For each interval  $i$ , we define the *minimal deployment*  $\check{D}^i$  as any feasible solution that uses the smallest possible number of machines:

$$\check{D}^i = \arg \min_{D^i} \left\{ \sum_{m,q} d_{m,q}^i \mid \min (4) \text{ s.t. } (5) - (7) \right\}.$$

We show, that both power attribution models yield  $\check{D}^i$ :

- *Feasibility with fewer machines is impossible:* If a solution  $\widehat{D}^i$  has fewer machines than  $\check{D}^i$  in at least one dimension, it would violate (6).
- *Using extra machines is suboptimal for time-based power attribution:* For  $\tilde{p}_{m,q}^i$ , any extra machine increases the objective by  $p_{m,q}^{\max}$ .

- *Using extra machines is suboptimal for utilization-based power attribution:* By Lemma 1, for  $p_{m,q}^i$  there is no incentive to deploy extra machines *of the same type*. If a quality tier  $q$  can be served by multiple machine types  $\widehat{\mathcal{M}}$ , under Assumption 3 (a strict ordering of these machines based on their idle and max power usage), if a more efficient machine type  $m_1$  is still able to carry extra load, using a less efficient type  $m_2$  instead can only increase the objective. Consequently, also across heterogeneous machine types, there is no incentive to add extra machines.

In either case (homogeneous or strictly ordered heterogeneous machines), any optimal solution must use exactly the minimal number of machines of each machine type. Because both the time-based and the utilization-based models thus select the same minimal deployment  $\check{D}^i$ , they yield equivalent optimal deployments.  $\square$